Intrinsic defect processes and elastic properties of Ti3AC2 (A = Al, Si, Ga, Ge, In, Sn) MAX phases

S.-R. G. Christopoulos, P. P. Filippatos, M. A. Hadi, N. Kelaidis, M. E. Fitzpatrick, and A. Chroneos

Original citation:
S.-R. G. Christopoulos, P. P. Filippatos, M. A. Hadi, N. Kelaidis, M. E. Fitzpatrick, and A. Chroneos (2018) Intrinsic defect processes and elastic properties of Ti3AC2 (A = Al, Si, Ga, Ge, In, Sn) MAX phases. *Journal of Applied Physics* (123) 2, 025103. DOI: 10.1063/1.5011374

https://doi.org/10.1063/1.5011374

Intrinsic defect processes and elastic properties of Ti_3AC_2 (A = Al, Si, Ga, Ge, In, Sn) MAX phases

S.-R. G. Christopoulos, P. P. Filippatos, M. A. Hadi, N. Kelaidis, M. E. Fitzpatrick, and A. Chroneos

Citation: Journal of Applied Physics **123**, 025103 (2018);
View online: https://doi.org/10.1063/1.5011374
View Table of Contents: http://aip.scitation.org/toc/jap/123/2
Published by the American Institute of Physics

Intrinsic defect processes and elastic properties of Ti_3AC_2 (A = Al, Si, Ga, Ge, In, Sn) MAX phases

S.-R. G. Christopoulos,[1] P. P. Filippatos,[2] M. A. Hadi,[3] N. Kelaidis,[1] M. E. Fitzpatrick,[1] and A. Chroneos[1,a)]

[1]*Faculty of Engineering, Environment and Computing, Coventry University, Priory Street, Coventry CV1 5FB, United Kingdom*
[2]*Department of Electrical and Computer Engineering, National Technical University of Athens, 9 Iroon Polytechniou Str., Zografou 15780, Greece*
[3]*Department of Physics, University of Rajshahi, Rajshahi 6205, Bangladesh*

(Received 31 October 2017; accepted 21 December 2017; published online 9 January 2018)

$M_{n+1}AX_n$ phases (M = early transition metal; A = group 13–16 element and X = C or N) have a combination of advantageous metallic and ceramic properties, and are being considered for structural applications particularly where high thermal conductivity and operating temperature are the primary drivers: for example in nuclear fuel cladding. Here, we employ density functional theory calculations to investigate the intrinsic defect processes and mechanical behaviour of a range of Ti_3AC_2 phases (A = Al, Si, Ga, Ge, In, Sn). Based on the intrinsic defect reaction, it is calculated that Ti_3SnC_2 is the more radiation-tolerant 312 MAX phase considered herein. In this material, the C Frenkel reaction is the lowest energy intrinsic defect mechanism with 5.50 eV. When considering the elastic properties of the aforementioned MAX phases, Ti_3SiC_2 is the hardest and Ti_3SnC_2 is the softest. All the MAX phases considered here are non-central force solids and brittle in nature. Ti_3SiC_2 is elastically more anisotropic and Ti_3AlC_2 is nearly isotropic. *Published by AIP Publishing*. https://doi.org/10.1063/1.5011374

I. INTRODUCTION

The unusual combination of thermophysical properties of $M_{n+1}AX_n$ phases (M = early transition metal, A = 13–16 element and X = C or N) constitute them as potential materials in high temperature applications. They were first synthesized by Nowotny,[1] but the investigations of Barsoum *et al.*,[2,3] which highlighted the common properties of the phases, were the ones to capture the interest of the community. The detection of the exceptional properties of Ti_3SiC_2 and the potential for technological applications, on the basis of their partially metallic and partially ceramic properties, has led to the synthesis of numerous MAX phases. For example, they combine good machinability, high thermal shock resistance, high elastic stiffness, high melting temperature, and high thermal and electrical conductivity.[2–5] The metallic and ceramic properties in the MAX phases are linked to their crystal structure, consisting of the stacking of *n* "ceramic" layer(s) interleaved by an A "metallic" layer as shown in Fig. 1.[2–5] $M_{n+1}AX_n$ phases belong to the $P6_3/mmc$ space group (no. 194).[1,2] The first (n = 1) and second (n = 2) members of the family are referred to as the 211 and 312 MAX phases.

Figure 1 shows the crystal structure of the 312 MAX phases.[1,2] They are characterized by a highly symmetric unit cell with atomic layers stacked along the *c*-direction. The M layers enclose an X layer forming an M_2X slab that has a face-centred-cubic-type stacking sequence, whereas the A layers effectively separate these slabs. Additionally, the stacking around the A layers has an HCP pattern, with the A layers forming a mirror plane in the crystal.

Besides Ti_3SiC_2, other Ti-based MAX phases have attracted attention, such as Ti_3AlC_2. This compound has a better oxidation resistance in air than Ti_3SiC_2 due to the formation of a passivating Al_2O_3 outer layer.[6–8] The exceptional properties of the MAX phases have led to their consideration in a number of applications including batteries, electronic applications, and the passive safety protection of nuclear fuel cladding.[9–18] Furthermore, their combination of high-temperature stability, and radiation- and mechanical-damage-tolerance, combined with good machinability, has led to their development for structural components and parts for Gen IV nuclear reactor designs.[2]

The aim of the present study is to investigate the mechanical properties and the intrinsic defect processes of Ti_3AC_2 MAX phases (A = Al, Si, Ga, Ge, In, Sn): the study of the defect processes will be used to provide an initial screening criterion for radiation tolerance based on the Frenkel pair formation energies. There are a large number of possible MAX-phase compounds; therefore, through computational modelling of a broad spectrum of potential materials we aim to develop design rules that can guide experimental work and eventually tailor individual phase compositions to those with the most desirable properties.

II. METHODOLOGY

The plane wave density functional theory (DFT) code CASTEP[19,20] was used for all the calculations. Exchange and correlation interactions were formulated by employing the corrected density functional of Perdew, Burke and Ernzerhof (PBE)[21] in the generalized gradient approximation (GGA) and in conjunction with ultrasoft pseudopotentials.[22] For geometry

a)Author to whom correspondence should be addressed: ab8104@coventry.ac.uk

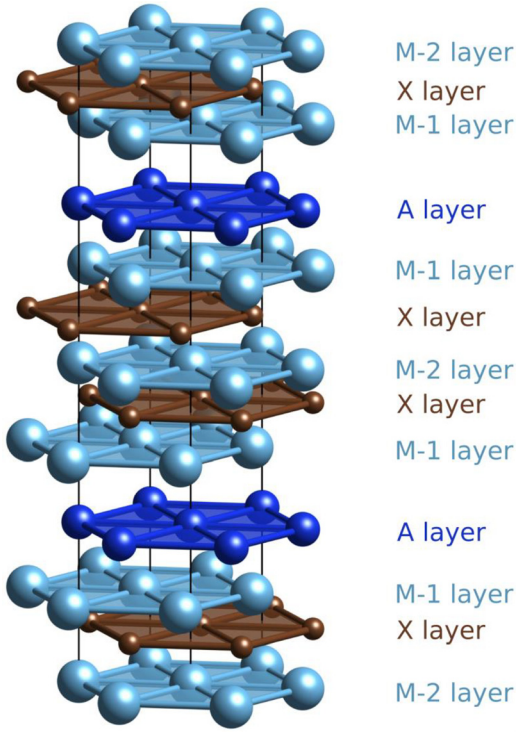

FIG. 1. Crystal structure of the M_3AX_2 phases.

optimization, we employed the Broyden–Fletcher–Goldfarb–Shanno (BFGS) minimiser. For the calculations of defect energies and interstitial sites, 108-atomic-site supercells (under constant pressure conditions), with a plane wave basis set cut-off of 450 eV and a $3 \times 3 \times 1$ Monkhorst-Pack (MP)[23] *k*-point grid, were used. The potential interstitial sites in the 312 MAX phases were previously reported;[9] however, we performed a comprehensive investigation to discover further potential interstitial sites. Considering a higher energy cut-off and/or more *k*-points changed defect energies by typically 0.01 eV. The elastic constants are calculated with modelling a conventional unit cell applying a plane wave energy cut-off of 550 eV and a $18 \times 18 \times 2$ k-point mesh according to the MP scheme. The efficacy and convergence of the approach as compared to experiment are also discussed in recent studies.[24–26]

III. RESULTS AND DISCUSSION

A. Frenkel defect formation

The investigation of the defect processes of the Ti_3AC_2 MAX phases relates to their potential nuclear applications. In that respect, it should be stressed that Ti_3InC_2 is only included for completeness and to derive trends as it is practically not applicable in nuclear applications due to the high cost and high neutron cross-section of indium. The calculation of the energetics of Frenkel defects is important particularly for nuclear applications, because a low pair formation energy can be associated with a higher content of more persistent defects, that in turn leads to the loss of ordering in the crystal structure. Radiation damage can be understood as an accumulation of defects that are formed by displacement cascades.[9,27,28] The

TABLE I. The preferable interstitial sites for the Ti_3AC_2 MAX phases (A = Al, Si, Ga, Ge, In, Sn).

Phases	Ti_i	A_i	C_i
Ti_3SiC_2	3/4, 0.70175, 1/4	2/3, 1/3, 1/4	1/3, 2/3, 1/4
Ti_3AlC_2	0.27651, 0.28686, 1/4	2/3, 1/3, 1/4	1/3, 2/3, 1/4
Ti_3SnC_2	1/3, 2/3. 0.69831	0.52046, 0.48794, 0.29530	1/3, 2/3, 0.65221
Ti_3GeC_2	3/4, 2/3, 1/4	2/3, 1/3, 1/4	1/3, 2/3, 1/4
Ti_3GaC_2	–0.01732, 0.28892, 1/4	0.34145, 0.67238, 3/4	1/3, 2/3, 1/4
Ti_3InC_2	2/3, 1/3, 0.30659	1/3, 2/3, 0.71352	1/3, 2/3, 0.65265

following relations are the three key Frenkel reactions in Kröger–Vink notation (in this notation V_A and A_i will denote a vacant A site and an A interstitial defect, respectively):[29]

$$Ti_{Ti} \rightarrow V_{Ti} + Ti_i, \quad (1)$$

$$A_A \rightarrow V_A + A_i, \quad (2)$$

$$C_C \rightarrow V_C + C_i. \quad (3)$$

In 312 MAX phases, there exist numerous possible interstitial sites.[9] For all the MAX phases considered herein, the preferable interstitials (Ti_i, A_i and C_i) are given in Table I. It can be observed that the most favourable interstitial sites vary, depending on the composition.

B. Antisite defect formation

It is common during radiation damage for the point defects formed to either recombine or occupy an alternative lattice site, forming what are known as antisite defects.[9] A low energy antisite formation energy implies that a significant population of residual defects will remain in the material, as the conversion of an interstitial into an antisite leads to a net reduction of defect mobility.[9,30] The antisite formation mechanisms are given by

$$Ti_{Ti} + A_A \rightarrow Ti_A + A_{Ti}, \quad (4)$$

$$Ti_{Ti} + C_C \rightarrow Ti_C + C_{Ti}, \quad (5)$$

$$A_A + C_C \rightarrow A_C + C_A. \quad (6)$$

C. Interaction of interstitials with vacancies

For interstitial defects forming in the Ti layer, the association with V_{Ti} needs to be considered

$$A_i + V_{Ti} \rightarrow A_{Ti}, \quad (7)$$

$$C_i + V_{Ti} \rightarrow C_{Ti}. \quad (8)$$

For interstitial defects forming in the A layer

$$Ti_i + V_A \rightarrow Ti_A, \quad (9)$$

$$C_i + V_A \rightarrow C_A. \quad (10)$$

Finally, for interstitial defects forming in the C layer

$$Ti_i + V_C \rightarrow Ti_C, \quad (11)$$

$$A_i + V_C \rightarrow A_C. \quad (12)$$

Essentially, these relations reveal whether interstitial defects recombine with vacancies to form antisite defects or remain as isolated interstitials.

D. Displacement of lattice atoms by interstitials

Following displacement cascades, there is a hyperstoichiometry of interstitials that can potentially lead to the displacement of atoms from their lattice sites to interstitial sites. This in turn may encourage the formation of antisite defects. A typical example is γ-TiAl where $Ti_i + Al_{Al} \rightarrow Ti_{Al} + Al_i$ leads to the reduction of the unfavourable Ti_i with a concurrent increase of the concentration of $Ti_{Al} + Al_i$.[30] In 312 MAX phases, such as Ti_3SiC_2, analogous reactions were energetically unfavorable.[9] Finally, reactions 13–18 will be considered

$$Ti_i + A_A \rightarrow Ti_A + A_i, \quad (13)$$

$$Ti_i + C_C \rightarrow Ti_C + C_i, \quad (14)$$

$$A_i + Ti_{Ti} \rightarrow A_{Ti} + Ti_i, \quad (15)$$

$$A_i + C_C \rightarrow A_C + C_i, \quad (16)$$

$$C_i + Ti_{Ti} \rightarrow C_{Ti} + Ti_i, \quad (17)$$

$$C_i + A_A \rightarrow C_A + A_i. \quad (18)$$

E. Implications of defect processes

In previous studies, it has been considered that the radiation performance of materials relies on their propensity to form and accommodate point defects. The accumulation of defects can lead to the destabilization of the material, leading to volume changes and microcracking.[31,32] Displacive radiation leads to an athermal concentration of Frenkel pairs, while it has been argued that the radiation tolerance of materials relies upon the resistance to form persistent populations of Frenkel (and antisite) defects.[28] In this framework, a high defect energy is an indication of radiation tolerance.

Previous experimental studies[33,34] determined that Ti_3AlC_2 is more tolerant to radiation damage in comparison to Ti_3SiC_2. Based on the defect processes investigated by DFT (refer to Table II), it can be concluded that Ti_3SnC_2 is the most radiation tolerant MAX phase considered here. This is because the lowest energy Frenkel intrinsic disorder mechanism (relation 3, Frenkel reaction with 5.50 eV) in Ti_3SnC_2 is higher in energy compared to the lowest energy intrinsic disorder mechanisms of the other MAX phases considered here although the respective energy for Ti_3InC_2 differs by only 0.35 eV (refer to Table II). This in turn implies that there will be a lower concentration of Frenkel defects in Ti_3SnC_2, which is beneficial for its radiation tolerance.[28] Considering also the antisite defect reactions, the relation 4 (i.e., the production of $Ti_A + A_{Ti}$) is the lowest energy process for Ti_3SnC_2 with 5.38 eV i.e., only 0.23 eV higher than the carbon Frenkel reaction in Ti_3InC_2. Nevertheless, considering the high cost and high neutron cross-section of indium Ti_3SnC_2 is the better candidate.

Although Eq. (7) implies that Ti interstitials will recombine with V_A to form Ti_A antisites, for all the 312 MAX phases considered, there will be a very small concentration of Ti_i in the first place due to very high reaction energies for Eq. (1) as listed in Table II. This will effectively render Eq. (7) practically irrelevant under equilibrium conditions. Similar arguments are also valid for the other antisite reactions [Eqs. (8) and (9)]. These reactions may become relevant when considering a non-equilibrium environment (i.e., under irradiation) where an increased defect concentration is possible. In such conditions, it is anticipated that Ti_i will recombine with V_A to produce Ti_A antisites. Also, the production of C_A via Eq. (8) should be expected for Ti_3AC_2 (A = Ga, Ge, In, Sn). These processes may only be relevant after irradiation, given that the formation of the Ti_i defects via the Frenkel reaction (relation 1) is high for all the 312

TABLE II. The calculated defect reaction energies (in eV, for relations 1–18) for the Ti_3AC_2 MAX phases (A = Al, Si, Ga, Ge, In, Sn).

Reaction	Ti_3AlC_2	Ti_3SiC_2	Ti_3GaC_2	Ti_3GeC_2	Ti_3InC_2	Ti_3SnC_2
(1) $Ti_{Ti} \rightarrow V_{Ti} + Ti_i$	7.32	7.30	7.43	7.82	9.71	9.40
(2) $A_A \rightarrow V_A + A_i$	3.40	3.19	3.31	4.95	7.23	9.41
(3) $C_C \rightarrow V_C + C_i$	3.17	3.09	4.27	4.38	5.15	5.50
(4) $Ti_{Ti} + A_A \rightarrow Ti_A + A_{Ti}$	3.27	4.65	5.03	5.80	5.33	5.38
(5) $Ti_{Ti} + C_C \rightarrow Ti_C + C_{Ti}$	10.52	13.44	11.76	12.82	12.97	12.13
(6) $A_A + C_C \rightarrow A_C + C_A$	9.26	6.28	8.24	7.05	11.14	10.18
(7) $A_i + V_{Ti} \rightarrow A_{Ti}$	–4.20	–3.15	–2.94	–3.09	–6.39	–7.36
(8) $C_i + V_{Ti} \rightarrow C_{Ti}$	–0.48	–0.41	–1.45	–1.14	–1.84	–1.75
(9) $Ti_i + V_A \rightarrow Ti_A$	–3.25	–2.69	–2.78	–3.88	–5.22	–6.07
(10) $C_i + V_A \rightarrow C_A$	0.31	0.06	–0.75	–0.45	–0.10	–0.07
(11) $Ti_i + V_C \rightarrow Ti_C$	0.51	3.45	1.51	1.77	–0.05	–1.02
(12) $A_i + V_C \rightarrow A_C$	2.39	–0.06	1.41	–1.83	–1.14	–4.65
(13) $Ti_i + A_A \rightarrow Ti_A + A_i$	0.15	0.50	0.54	1.07	2.01	3.34
(14) $Ti_i + C_C \rightarrow Ti_C + C_i$	3.68	6.54	5.78	6.15	5.10	4.48
(15) $A_i + Ti_i \rightarrow A_{Ti} + Ti_i$	3.12	4.16	4.49	4.73	3.32	2.04
(16) $A_i + C_C \rightarrow A_C + C_i$	5.55	3.03	5.68	2.55	4.01	0.85
(17) $C_i + Ti_{Ti} \rightarrow C_{Ti} + Ti_i$	6.84	6.89	5.98	6.68	7.87	7.65
(18) $C_i + A_A \rightarrow C_A + A_i$	3.71	3.25	2.56	4.50	7.13	9.34

TABLE III. The calculated results for the elastic constants C_{ij} (GPa), bulk modulus B (GPa), shear modulus G (GPa), Young's modulus Y (GPa), Poisson's ratio v, Pugh's ratio B/G, elastic anisotropy factor A, and shear anisotropy factor (k_c/k_a) for the Ti_3AC_2 MAX phases (A = Al, Si, Ga, Ge, In, Sn). All elastic constants and moduli are shown in round figure; all factors and ratios are taken to four decimal.

Phase	c_{11}	c_{12}	c_{13}	c_{33}	c_{44}	A	k_c/k_a	B	G	Y	B/G	v	References
Ti_3AlC_2	355	74	66	295	125	0.9709	1.3142	157	131	307	1.1985	0.1736	This
	361	75	70	299	124	0.9538	1.2926	160	131	309	1.2214	0.1784	37
	368	81	76	313	130	0.9830	1.2532	168	135	320	1.2445	0.1831	37
	358	84	75	293	122	0.9738	1.3429	163	127	303	1.2790	0.1899	36
	…	…	…	…	…	…	…	165	124	297	1.3306	0.20	39
Ti_3SiC_2	365	89	99	352	156	1.2023	1.0119	184	143	341	1.2867	0.1914	This
	370	99	111	349	151	1.2090	1.0382	192	138	334	1.3918	0.2102	36
	372	88	98.3	352.6	167	1.2674	1.0358	185	149	352	1.2449	0.1832	38
	…	…	…	…	…	…	…	185	139	333	1.3309	0.20	39
	…	…	…	…	…	…	…	185.6	143.8	343	1.2906	0.192	40
Ti_3GeC_2	356	88	91	324	140	1.1245	1.1245	175	134	320	1.3060	0.1950	This
	357	100	97	325	129	1.0508	1.1524	180	126	307	1.4263	0.2159	36
	355.4	85.2	94	338	148	1.1714	1.0323	177	138	312	1.2826	0.2068	38
Ti_3SnC_2	319	103	80	304	113	0.9762	1.1696	163	112	273	1.4554	0.2205	This
	331	96	80	285	108	0.9431	1.3023	161	113	274	1.4315	0.2167	36
	331	91	81	299	129	1.1026	1.1932	162	122	285	1.3279	0.2082	38
Ti_3InC_2	338	80	63	276	92	0.7541	1.3709	151	111	267	1.3604	0.2048	This
	340	85	67	263	97	0.8255	1.4778	152	111	267	1.3619	0.2051	36
Ti_3GaC_2	359	78	69	292	123	0.9591	1.3408	159	130	306	1.2231	0.1787	This
	356	86	75	285	113	0.9199	1.3899	162	122	293	1.3235	0.1982	36

MAX phases considered here (7.30–9.71 eV, refer to Table II). The processes considered for the displacement of lattice atoms by interstitials are all positive in energy. From an experimental viewpoint, the radiation tolerance and oxidation resistance at high temperature of Ti_3SnC_2 have to be determined.

F. Elastic properties

Elastic constants of Ti_3AC_2 are important as we can derive useful information about their mechanical properties. As the Ti_3AC_2 MAX phases have hexagonal crystal structures, they will have five independent elastic constants (c_{11}, c_{12}, c_{13}, c_{33}, c_{44}), and $c_{66} = (c_{11}–c_{12})/2$. For crystal stability, the following conditions must be met:[35]

$$c_{11} > 0, \quad c_{33} > 0, \quad c_{44} > 0, \quad (c_{11} + c_{12})c_{33} > 2(c_{13})^2 \quad \text{and} \quad (c_{11} - c_{12}) > 0. \tag{19}$$

The calculated results for the Ti_3AC_2 MAX phases considered here are given in Table III (refer also to Refs. 36–40) where we can observe that the above conditions are satisfied. The present results are within a few percent different and thus in excellent agreement as compared with previous experimental and DFT results (for example Refs. 36–40).

Ti_3SiC_2 is the hardest, whereasTi_3SnC_2 and Ti_3InC_2 are the softest and thus the more easily machinable of the Ti_3AC_2 phases considered herein (although all MAX phases considered should be relatively easy machinable and this is not a factor that would hinder industrial processes). From the values of Table III, it is expected that the deformation of Ti_3InC_2 is easier than the other Ti_3AC_2 phases. The c_{12} elastic constant for Ti_3AlC_2 reveals that it deforms more easily as compared to Ti_3SiC_2, Ti_3GeC_2, Ti_3GaC_2, Ti_3SnC_2, and Ti_3InC_2 in the (110) plane along the ⟨100⟩ direction. The low c_{12}, c_{13} values of the Ti_3AlC_2, Ti_3InC_2, and Ti_3GaC_2 indicate that when we apply a force in the a-axis of the crystal, these materials will be easier to shear at the b- and c-axis. The lower value of the elastic constant c_{33} of Ti_3InC_2 makes it relatively easier (as compared to the other MAX phases considered here) to compress in the ⟨001⟩ direction under uniaxial stress. It should be noted, however, that it is considerably higher than most structural materials. Figure 2(a) represents the dependence of the c_{ij} on the atomic radius of the A-elements.

In Table III, we have also listed the bulk modulus, shear modulus, and the Young's modulus. The Bulk modulus B is a measure of the resistance under compression. The replacement of the A-element with In results in the lowest bulk modulus (refer to Table III); therefore, Ti_3InC_2 has a lower resistance to compression. Conversely, Ti_3SiC_2 has the highest value; thus, it is more resistant to high pressure. The shear modulus, G, represents the resistance of the material to shape change. Ti_3InC_2 has the lowest G, which means that a shape change in Ti_3InC_2 is easier than the other Ti_3AC_2 phases. Finally, the Young's modulus, E, is a measure of the stiffness of a material. Of the MAX Phases considered, Ti_3SiC_2 requires more stress to deform, and Ti_3InC_2 requires low stress as compared to other MAX phases listed in Table III. Figure 2(b) represents the bulk modulus, the shear modulus, and the Young's modulus as a function of the atomic radius of the A-elements.

To assess the failure modes of MAX Phases, we use Pugh's modulus (B/G), which is linked to the brittle and ductile failure.[41] In particular, when the Pugh's modulus is higher than 1.75, the material is ductile, otherwise the material is brittle. All the Ti_3AC_2 MAX phases considered here are brittle (refer to Table III). The anisotropy factor, k_c/

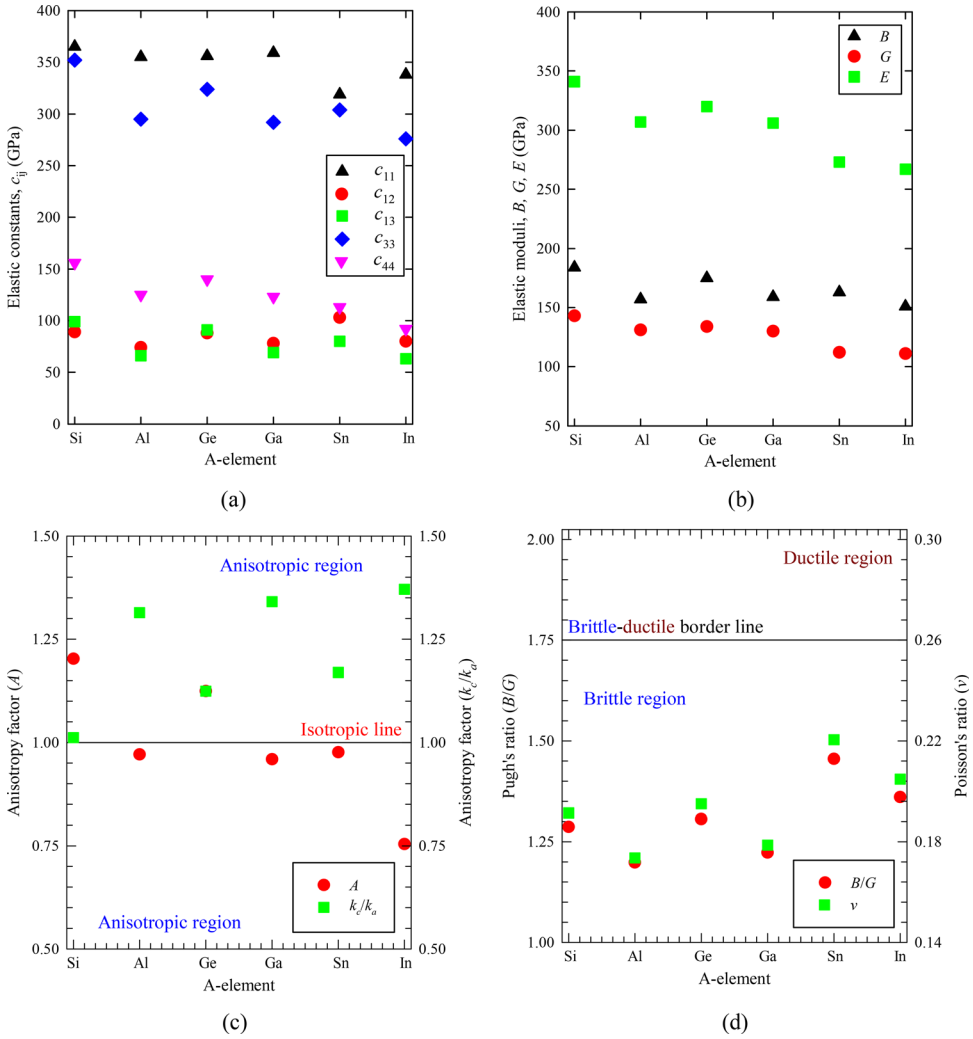

FIG. 2. (a) The elastic constants c_{ij}, (b) elastic moduli (B, G, E), (c) Pugh's and Poisson's ratios (B/G, ν), and (d) anisotropy factors (A, k_c/k_a) as a function of the atomic radius of A-element.

$k_a = (c_{11}+c_{12}-2c_{13})/(c_{33}-c_{13})$, reveals whether the material has a higher compressibility along the a-axis or the c-axis. According to the results in Table III, Ti_3SiC_2 is the only MAX phase that has compressibility on the a-axis almost the same as the one on the c-axis.

Another important parameter is Poisson's ratio. If the Poisson's constant is between 0.25 and 0.5, then the material is known as a central force solid, whereas otherwise it is a non-central force solid.[42] Similarly to Pugh's ratio, Poisson's ratio also categorizes the solids as brittle or ductile.[43] For a Poisson's ratio greater than 0.26, the solid is ductile, whereas if it is less than 0.26, it is brittle. In that respect, all the MAX phases considered here are non-central force solids and brittle in nature (refer to Table III). Figure 2(c) represents the Pugh's and Poisson's ratio as a function of atomic radius of A-element.

Elastic anisotropy is also an important descriptor about the nature of crystalline solids.[44] This elastic anisotropy may lead to an anisotropic thermal expansion and may create microcracks in the crystal formation. For hexagonal systems, the elastic anisotropy (A) is defined as: $A = 4c_{44}/(c_{11}+c_{33}-2c_{13})$. If $A \neq 1$, then the crystal is anisotropic. From Table III, it is observed that Ti_3SiC_2 and Ti_3InC_2 are elastically more anisotropic. The A-values of Ti_3AlC_2 are close to unity, indicating that the Al-based MAX phase is almost elastically isotropic. Figure 2(d) represents the dependence of elastic anisotropy factors on the A-element atomic radius.

IV. SUMMARY

The present study has considered the intrinsic defect processes and mechanical properties of Ti_3AC_2 (A = Al, Si, Ga, Ge, In, Sn) MAX phases. For these phases, the dominant intrinsic disorder mechanism was calculated to be the Frenkel reaction. The higher Frenkel energy for Ti_3SnC_2 implies superior radiation tolerance. In essence, we show that Ti_3SnC_2 merits systematic experimental and theoretical investigation as its properties should be superior, particularly in applications where radiation resistance is important. In the present study, the focus is on the defect reaction mechanisms and not on the influence of point defect concentration on the lattice stability. The latter can be important as it can affect the propensity of the MAX phase to amorphize under a radiation environment. Kinetics of the processes are bound to play a role and therefore, the migration energy barriers for

point defects (interstitial and vacancies) to diffuse and annihilate will need to be calculated. Among all the studied MAX phases, Ti_3SiC_2 is the hardest and Ti_3SnC_2 is the softest. All the Ti_3AC_2 phases are non-central force solids as well as brittle in nature. Ti_3AlC_2 is nearly isotropic and Ti_3SiC_2 is more anisotropic elastically.

ACKNOWLEDGMENTS

David Parfitt (Coventry University) is gratefully acknowledged for numerous discussions. S.-R.G.C., A.C., N.K., and M.E.F. are grateful for funding from the Lloyd's Register Foundation, a charitable foundation helping to protect life and property by supporting engineering-related education, public engagement, and the application of research.

[1]H. Nowotny, "Strukturchemie einiger verbindungen der ubergangsmetalle mit den elementen C, Si, Ge, Sn," Prog. Solid State Chem. **5**, 27–70 (1971).
[2]M. W. Barsoum and M. Radovic, "Elastic and mechanical properties of the MAX Phases," Annu. Rev. Mater. Res. **41**, 195–227 (2011).
[3]M. W. Barsoum and T. El-Raghy, "Synthesis and characterization of a remarkable ceramic: Ti_3SiC_2," J. Am. Ceram. Soc. **79**, 1953–1956 (1996).
[4]M. W. Barsoum, D. Brodkin, and T. El-Raghy, "Layered machinable ceramics for high temperature applications," Scr. Metall. Mater. **36**, 535–541 (1997).
[5]M. A. Hadi, S. H. Naqib, S.-R. G. Christopoulos, A. Chroneos, and A. K. M. A. Islam, J. Alloys. Compd. **724**, 1167 (2017).
[6]Z. J. Lin, M. S. Li, J. Y. Wang, and Y. C. Zhou, "High-temperature oxidation and hot corrosion of Cr_2AlC," Acta Mater. **55**, 6182–6191 (2007).
[7]S. Basu, N. Obando, A. Gowdy, I. Karaman, and M. Radovic, "Long-term oxidation of Ti_2AlC in air and water vapour at 1000-1300 °C temperature range," J. Electrochem. Soc. **159**, C90–C96 (2012).
[8]D. J. Tallman, B. Anasori, and M. W. Barsoum, "A critical review of the oxidation of Ti_2AlC, Ti_3AlC_2 and Cr_2AlC in air," Mater. Res. Lett. **1**, 115–125 (2013).
[9]S. C. Middleburgh, G. R. Lumpkin, and D. Riley, "Accommodation, accumulation, and migration of defects in Ti_3SiC_2 and Ti_3AlC_2 MAX phases," J. Am. Ceram. Soc. **96**, 3196–3201 (2013).
[10]D. Horlait, S. Grasso, A. Chroneos, and W. E. Lee, "Attempts to synthesise quaternary MAX phases $(Zr,M)_2AlC$ and $Zr_2(Al,A)C$ as a way to approach Zr_2AlC," Mater. Res. Lett. **4**, 137–144 (2016).
[11]D. Horlait, S. Grasso, N. Al Nasiri, P. A. Burr, and W. E. Lee, "Synthesis and high-temperature oxidation of MAX phases in the Cr-Ti-Al-C quaternary system," J. Am. Ceram. Soc. **99**, 682–690 (2016).
[12]V. Saltas, D. Horlait, E. N. Sgourou, F. Vallianatos, and A. Chroneos, Appl. Phys. Rev. **4**, 041301 (2017).
[13]D. Horlait, S. C. Middleburgh, A. Chroneos, and W. E. Lee, "Synthesis and DFT investigation of new bismuth-containing MAX phases," Sci. Rep. **6**, 18829 (2016).
[14]T. Lapauw *et al.*, "Synthesis of the novel Zr_3AlC_2 MAX phase," J. Eur. Ceram. Soc. **36**, 943–947 (2016).
[15]A. Talapatra *et al.*, "High-throughput combinatorial study of the effect of M site alloying on the solid solution behavior of M_2AlC MAX phases," Phys. Rev. B **94**, 104106 (2016).
[16]B. Tunca *et al.*, "Synthesis of MAX phases in the Zr-Ti-Al-C system," Inorg. Chem. **56**, 3489–3498 (2017).
[17]R. Arroyave *et al.*, "Does aluminium play well with others? Intrinsic Al-A alloying behavior in 211/312 MAX phases," Mater. Res. Lett. **5**, 170–178 (2017).
[18]M. A. Hadi, Y. Panayiotatos, and A. Chroneos, "Structural and optical properties of the recently synthesized $(Zr_{3-x}Ti_x)AlC_2$ MAX phases," J. Mater. Sci.: Mater. Electron. **28**, 3386–3393 (2017).
[19]M. C. Payne, M. P. Teter, D. C. Allan, T. A. Arias, and J. D. Joannopoulos, "Iterative minimization techniques for ab initio total-energy calculations: Molecular dynamics and conjugate gradients," Rev. Mod. Phys. **64**, 1045 (1992).
[20]M. D. Segall *et al.*, "First-principles simulation: Ideas, illustrations and the CASTEP code," J. Phys.: Condens. Matter **14**, 2717 (2002).
[21]J. Perdew, K. Burke, and M. Ernzerhof, "Generalized gradient approximation made simple," Phys. Rev. Lett. **77**, 3865 (1996).
[22]D. Vanderbilt, "Soft self-consistent pseudopotentials in a generalized eigenvalue formalism," Phys. Rev. B **41**, 7892 (1990).
[23]H. J. Monkhorst and J. D. Pack, "Special points for Brillouin-zone integrations," Phys. Rev. B **13**, 5188 (1976).
[24]M. A. Hadi, R. V. Vovk, and A. Chroneos, "Physical properties of the recently discovered $Zr_2(Al_{1-x}Bi_x)C$ MAX phases," J. Mater. Sci.: Mater. Electron. **27**, 11925–11933 (2016).
[25]E. Zapata-Solvas *et al.*, "Experimental synthesis and density functional theory investigation of radiation tolerance of $Zr_3(Al_{1-x}Si_x)C_2$ MAX phases," J. Am. Ceram. Soc. **100**, 1377–1387 (2017).
[26]E. Zapata-Solvas *et al.*, "Synthesis and physical properties of $(Zr_{1-x}Ti_x)AlC_2$ MAX phases," J. Am. Ceram. Soc. **100**, 3393–3401 (2017).
[27]J. B. Gibson, A. N. Goland, M. Milgram, and G. H. Vineyard, "Dynamics of radiation damage," Phys. Rev. **120**, 1229 (1960).
[28]K. E. Sickafus *et al.*, "Radiation tolerance of complex oxides," Science **289**, 748–751 (2000).
[29]F. A. Kröger and H. J. Vink, "Relations between the concentrations of imperfections in crystalline solids," Solid State Phys. **3**, 307–435 (1956).
[30]R. E. Voskoboinikov, G. R. Lumpkin, and S. C. Middleburgh, "Preferential formation of Al self-interstitial defects in γ-TiAl under irradiation," Intermetallics **32**, 230–232 (2013).
[31]W. J. Weber, "Radiation-induced swelling and amorphization in $Ca_2Nd_8(SiO_4)_6O_2$," Radiat. Eff. **77**, 295–308 (1983).
[32]F. W. Clinard, Jr., D. L. Rohr, and R. B. Roof, "Structural damage in a self-irradiated zirconolite-based ceramic," Nucl. Instrum. Methods Phys. Res., Sec. B **1**, 581–586 (1984).
[33]K. R. Whittle *et al.*, "Radiation tolerance of $M_{n+1}AX_n$ phases, Ti_3AlC_2 and Ti_3SiC_2," Acta Mater. **58**, 4362–4368 (2010).
[34]X. M. Liu, M. Le Flem, J. L. Bechade, and I. Monnet, "Nanoindentation investigation of heavy ion irradiated $Ti_3(Si,Al)C_2$," J. Nucl. Mater. **401**, 149–153 (2010).
[35]M. Born, "On the stability of crystal lattices," Math. Proc. Cambridge Philos. Soc. **36**, 160–172 (1940).
[36]S. Aryal, R. Sakidja, M. W. Barsoum, and W.-Y. Ching, "A genomic approach to the stability, elastic, and electronic properties of the MAX phases," Phys. Status Solidi B **251**, 1480–1497 (2014).
[37]M. S. Ali, A. K. M. A. Islam, M. M. Hossain, and F. Parvin, Physica B **407**, 4221 (2012).
[38]W. Wang, L. Sun, Y. Yang, J. Dong, Z. Gu, and H. Jin, Results Phys. **7**, 1055 (2017).
[39]P. Finkel, M. W. Barsoum, and T. El-Raghy, J. Appl. Phys. **87**, 1701 (2000).
[40]M. Radovic, M. W. Barsoum, A. Ganguly, T. Zhen, P. Finkel, S. R. Kalidindi, and E. Lara-Curzio, Acta Mater. **54**, 2757 (2006).
[41]S. F. Pugh, "Relations between the elastic moduli and the plastic properties of polycrystalline pure metals," Philos. Mag. **45**, 823–843 (1954).
[42]O. L. Anderson and H. H. Demarest, Jr., "Elastic constants of the central force model for cubic structures: Polycrystalline aggregates and instabilities," J. Geophys. Res. **76**, 1349–1369, https://doi.org/10.1029/JB076i005p01349 (1971).
[43]I. N. Frantsevich, F. F. Voronov, and S. A. Bokuta, *Elastic Constants and Elastic Moduli of Metals and Insulators Handbook* (Naukova Dumka, Kiev, 1983), pp. 60–180.
[44]G. Vaitheeswaran, V. Kanchana, A. Svane, and A. Delin, "Elastic properties of $MgCNi_3$ - A superconducting perovskite," J. Phys.: Condens. Matter **19**, 326214 (2007).